Available online at www.sciencedirect.com
ScienceDirect
Energy Reports 8 (2022) 672–683
www.elsevier.com/locate/egyr

2021 8th International Conference on Power and Energy Systems Engineering (CPESE 2021), 10–12 September 2021, Fukuoka, Japan

WAMS based Thevenin Index for voltage stability assessment with increasing wind power penetration and additional distributed load

Raju Chintakindi*, Pradyumna Pradhan, Arghya Mitra

Visvesvaraya National Institute of Technology, Nagpur, 440010, India

Received 31 October 2021; accepted 9 November 2021
Available online 3 December 2021

Abstract

One of the major concerns about the growing penetration of renewable energy into the power network is the analysis of the impact of such penetration on system stability. The Local Thevenin Index (LTI) based on the Wide Area Monitoring System (WAMS) is a novel technique in scientific research to assess the voltage stability of power systems integrated with renewable energy. From the standpoint of grid voltage stability, this index aids in determining the best location for integrating the wind farm into the existing power system. The effect of a significant penetration of doubly-fed induction generator (DFIG) based wind farms on the voltage stability of a large power network is analyzed in this research. The novelty of this research is to find the effect of the rise in wind power penetration level and additional distributed loads on a wind farm integrated large power system for voltage stability analysis. The MATLAB-Simulink platform is used to validate the proposed work with the New England 16-machine 68-bus power system.

Peer-review under responsibility of the scientific committee of the 8th International Conference on Power and Energy Systems Engineering, CPESE, 2021.

Keywords: WAMS; Phasor measurement unit; Voltage stability; DFIG based wind farm; Local Thevenin Index

1. Introduction

Sustainable energy sources such as solar photovoltaics and wind power are increasingly being integrated into the system because of the depletion of fossil fuel reserves and their associated environmental effects. Wind power is one of the fastest growing of all renewable resources and is still emerging as one of the largest rising green technologies in the contemporary energy sector. Because these energy sources are unpredictable and highly variable in nature, they raise concerns about the existing power grid's stability. However, on the other hand, accelerating pressure on power-grid facility providers to maximize the use of existing services and infrastructure could cause issues with long-term voltage stability analysis. To improve operational responsiveness, smart-grid operators are using Synchrophasor technology to implement new measurement concepts for wide-area monitoring systems and

* Corresponding author.
E-mail address: rajuphdvnit@gmail.com (R. Chintakindi).

https://doi.org/10.1016/j.egyr.2021.11.215

Peer-review under responsibility of the scientific committee of the 8th International Conference on Power and Energy Systems Engineering, CPESE, 2021.

Nomenclature

WAMS	Wide-area Monitoring Systems
PMU	Phasor Measurement Unit
PMUT	Phasor Measurement Unit Technology
VSI	Voltage Stability Indices
LTI	Local Thevenin Index
WSCC	Western System Coordinating Council
DFIG	Doubly Fed Induction Generator
WT	Wind Turbine
STI	Sensitivity based Thevenin Index
RSC	Rotor Side Converter
GSC	Grid Side Converter
GPS	Global Positioning System
PDC	Phasor Data Concentrator
PPS	Pulse Per Second

smart automation (WAMSA). WAMSA is a cutting-edge technology that measures and records real-time power network variables, allowing for the detection of system stability and potential threats, as well as assisting in the planning and implementation of prevention strategies [1] . The Synchrophasor is used to improve grid efficiency by detecting faults and unstable conditions from time to time. The widespread adoption of Phasor Measurement Units (PMU) has aided the development of some voltage stability indices (VSIs), which are used to monitor the system's long-term voltage stability in real-time applications [2].

At a bus terminal, the Local Thevenin Index (LTI) is identified by calculating the Thevenin-Equivalent (TE) from time-synchronized phasor voltage and/or current measurements [3]. The reliability of the LTI estimation has aided its implementation process, and multiple regulation systems based on priorities, such as determining whether the power-grid is far from crashing, are being evaluated [4]. A WAMS voltage profile dataset could be used to validate the LTI, which is recorded on the PMUs. Since, this LTI is quantified by using the Synchrophasor database in real-time, sometimes it is typically distorted by noise, and the grid operator is unable to activate the control scheme within the period specified. To address this issue, the sensitivity-focused Thevenin-index (STI) was proposed as a means of verifying the LTI in the control center [3]. The synchronized phasor samples can be used to compute a variety of bus voltage indices, the most common of which are Thevenin equivalents based on VSIs.

A primary research for the modeling and simulation of DFIG-based wind farm connected to the WSCC 9-bus system was conducted to find a WAMS-based Thevenin-index (LTI) for the voltage stability analysis [5]. This research presents LTI to investigate the impact of wind energy integration into a multi-machine power systems, aiming for a best possible location from absolute grid voltage stability. Also the study was carried out to investigate the optimum wind power penetration from voltage stability point of view using the same LTI. The same study is extended for a large power system (16-machine 68-bus system) to find the best location and optimum wind power penetration at that location. For the previous study in 9-bus system, an additional load of same value as the wind farm output power was connected at the DFIG terminal bus in order to keep the steady state load flow of the system unchanged even after wind farm integration. But, from practical point of consideration, this additional load demand may be distributed among the nearby load buses of the system. So, the study is carried out further by considering this distributed load case in 9-bus system as well as 68-bus system.

The following is the format of this article: Section 2 describes briefly about the system with real-time wide-area measurement using Synchrophasor technology and also about the DFIG-based windmills into the power grid. Section 3 explains the computation of the Local Thevenin Index (LTI). Section 4 explores the study of system voltage stability with varying wind farm locations and addresses the effect of the rise in wind power penetration levels on the system's voltage stability with concentrated additional load case in 68-bus system. Further, it analyses the system voltage stability assessment with distributed additional load case in both 9-bus and 68-bus system. The paper ends with its conclusive remarks.

2. Overview of real-time wide-area measurement system and DFIG-based wind farm

2.1. Time synchronized real-time wide-area measurement system

Power engineers are started depending on the use of wide-area measurement techniques with sophisticated control and prevention technology. WAMS incorporates the functions of both conventional and emerging metering processes with the interface of power grids to measure, coordinate, and control power providers across a large geographical area. Fig. 1 shows the coordination of PMUs in defined load buses, including industrial sector, agricultural sector, and residential buildings, through GPS signal based on the Synchrophasor technology perception.

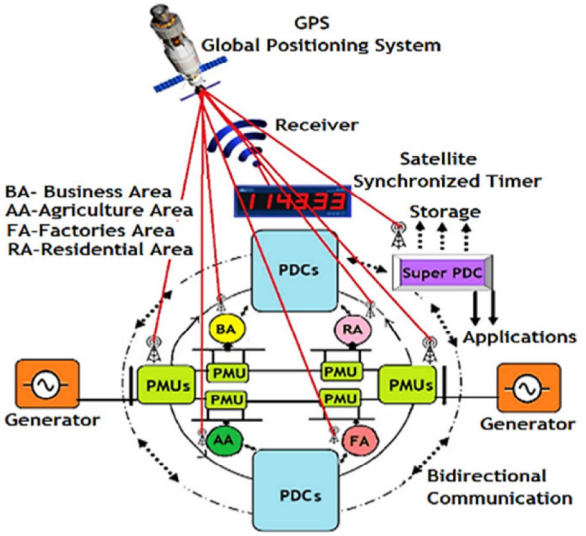

Fig. 1. Real-time wide-area measurement system with GPS time synchronization technology [6].

2.2. DFIG-based wind farm integration into the power grid

The primary factor in the constant voltage issue has been the transaction of reactive power with the electrical network. The ability of a DFIG to produce more output than its maximum capacity without overheating could be extremely advantageous [7]. DFIG offers a viable option for variable speed configurations that require a variable-speed range of around ±30% of synchronous speed [8]. In DFIG-based wind farm, the use of the DFIG functionality curve to impose rotor and stator current limits was discussed in [9]. A standard second-order induction-machine model (IMM) is used to model the DFIG. This model considers all relevant components that affect the dynamic characteristics of DFIGs, including the rotor side converter (RSC), which controls the rotor voltage [10]. A transformer and dual-circuit section are used to integrate a DFIG into a network load terminal [11]. A multi-machine power system has been embedded with a high-power DFIG oriented wind farm as shown in Fig. 2. The wind turbine is connected to the DFIG via a drivetrain with a gearbox of ratio n_s. P_s and Q_s denote the active and reactive power that flows through the stator windings. Similarly, the active and reactive powers P_r and Q_r flow through the rotor circuit, accounting for approximately 30% of the total power rating. The wind speed was set at 15 m/s for this investigation. The overall active and reactive power exchanged by the wind farm in a power network can be calculated by using the Eqs. (1) and (2).

$$P_{tot} = P_s + P_r = V_{ds} i_{ds} + V_{qs} i_{qs} + V_{dr} i_{dr} + V_{qr} i_{qr} \tag{1}$$

$$Q_{tot} = Q_s + Q_{GSC} = V_{qs} i_{ds} - V_{ds} i_{qs} \tag{2}$$

Here, V_{qs}, V_{ds}&V_{qr}, V_{dr} are the q-axis & d-axis voltage profiles of the stator and rotor circuits accordingly; similarly, i_{qs}, i_{ds}&i_{qr}, i_{dr} are the q-axis & d-axis current profiles of the stator and circuits; Q_{GSC} is the grid-side converter reactive-power.

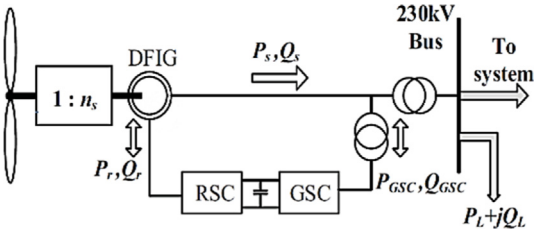

Fig. 2. DFIG connection to the system load bus.

3. Computation of the Local Thevenin Index (LTI)

LTI is assessed on a load bus using localized phasor measurement of voltage and/or current. The industrial application of LTI computation is greatly enhanced by its simplicity. In addition, depending on the LTI's characteristics, it has implemented a variety of mitigation measures to prevent the grid from collapsing [12]. The LTI computation is described in detail in [13]. The LTI is defined as the absolute value of the ratio of estimated Thevenin-impedance (Z_{th}) to Load-impedance (Z_L) at a load bus (ith bus) terminal, as presented in Eqs. (3) to (5). The Thevenin-impedance is calculated using two successive phasor voltage and/or current measurement with the assumption that the equivalent variables do not alter during the time interval in between the two measurements. The statement is true whenever the load increment ($\Delta\lambda$) between these two consecutive measurements is quite small.

$$Z_{thi} = \frac{V_i^{(2)} - V_i^{(1)}}{I_i^{(2)} - I_i^{(1)}} = \frac{\Delta V_i}{\Delta I_i} \tag{3}$$

$$Z_{Li} = \frac{V_i^{(1)}}{I_i^{(1)}} \tag{4}$$

$$LTI_i = \left|\frac{Z_{thi}}{Z_{Li}}\right| \tag{5}$$

Here, $V_i^{(1)}$ and $I_i^{(1)}$ are the corresponding points to the voltage and/or current phasors measured at the first instant, i.e. the initial stable position. $V_i^{(2)}$ and $I_i^{(2)}$ are the corresponding points to the voltage and current phasors measured at the second instant, i.e. after increment of load, and 'i' denote the load bus number. The LTI value rises with the increase in load. The LTI quantity is close to zero light loads and close to one when under heavy loads. The LTI with a value less than 1 means that the system is at a desired operating state. Therefore, it can be stated that a system with lower LTI values is generally more stable than the system with higher LTI values.

4. Voltage stability assessment using LTI

Voltage stability refers to the ability of a power system to maintain steady state voltages across all buses during normal operation and after a disturbance. The term "steady state voltage" refers to keeping voltages within a certain range. Voltage instability is a serious power system problem that occurs when the voltage of some buses in a power system exceeds the specified limit. LTI is one of the voltage stability indicators that tracks the system's long-term voltage stability using WAMS measurements.

From the base study using 9-bus system, bus 8 (one of the load buses) was found to be the best location for wind farm integration and the optimum wind power penetration at that location was found to be 90 MW [5]. Further, the investigation was carried out by focusing on large power systems such as New England's 16-machine 68-bus power system [14]. Generally, in the case of such large systems, the disturbance occurring at a specific location affects the neighboring buses only. Considering this factor, all the buses in the 68-bus system are divided into different small groups of buses based on nearness, which are considered as four different zones [15]. Zone I : 67, 68, 37, 52, 19, 20, 21, 22, 23, 24, 27, 4, 5, 6, 7. Zone II : 56, 57, 58, 59, 60, 61, 62, 63, 64, 65, 66, 2, 3. Zone III : 53, 54, 55, 37, 52, 25, 26, 27, 28, 29, 1, 8, 9. Zone IV : 53, 61, 30, 31, 32, 33, 34, 35, 36, 17, 10, 11, 12. The 16-machine, 68-bus system is schematically represented in Fig. 3. Fig. 4 represents the 9-bus system.

The study is carried out in each zone by assuming some available points of connection for wind farm integration. We have to find the best location, out of these selected points of connections, from system voltage stability point

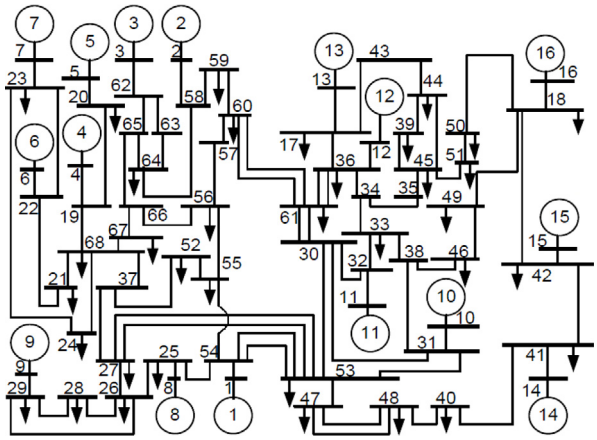

Fig. 3. Schematic representation of the 16-machine 68-bus framework.

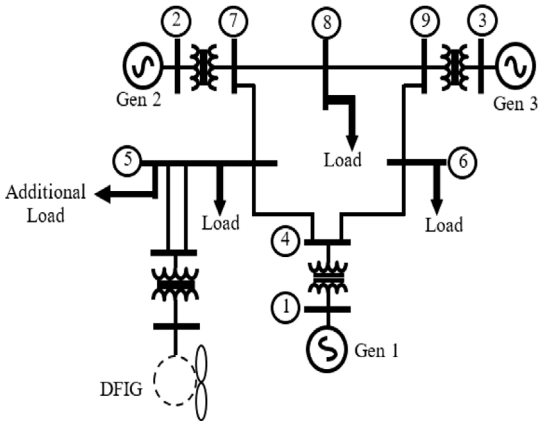

Fig. 4. WSCC 3-machine 9-bus power system.

of view. Here, an aggregated model of wind farm is considered which consists of a large number of wind turbine-generator sets. In each turbine-generator set, the wind speed is kept constant at a rated speed of 15 m/s (DFIG is operated in a super synchronous mode) and each DFIG generates 1.5 MW of output power. Reactive power generation is maintained at 0 MVar. The wind farm has a capacity of 1000 MW. The system has a base capacity of 100 MVA. An additional load is considered to be connected to the DFIG terminal bus and its value is made equal to the power produced by the DFIG. So, there would be no change in the steady state load flow of the system even after wind farm integration [16]. The main focus of the study is to show the effectiveness of the WAMS based LTI: (a) to determine the best location for the wind farm integration, and (b) to find the optimum wind penetration at that best location to have maximum voltage stability of the system.

4.1. Identifying the best location for wind farm integration

First, the study is carried out in zone-I by assuming that the possible points of connection for wind farm integration are bus 52, bus 67, and bus 68. The wind farm is integrated at these three locations one by one and the LTI is calculated at the three load buses for 1% to 5% of load increment. The LTI results are shown in Table 1. It can be observed that the LTI values of the load buses are varying with changes in wind farm locations, which indicates a variation in the steady state voltage stability of the system. We are getting least LTI values at the load buses for the case of wind farm integration at bus 68 compare to the other two points of wind farm integration. This can be clearly visualized in the LTI plots, which are shown in Figs. 5 to 7. So the system is relatively more

Table 1. Variation of LTI for different wind farm locations.

Wind farm location	LTI with different $\Delta\lambda$					
	Bus	$\Delta\lambda$				
		0.01	0.02	0.03	0.04	0.05
Bus 52	52	0.568	0.570	0.573	0.575	0.579
	67	0.515	0.518	0.520	0.524	0.526
	68	0.487	0.491	0.493	0.496	0.498
Bus 67	52	0.518	0.521	0.523	0.525	0.528
	67	0.452	0.454	0.457	0.459	0.464
	68	0.423	0.426	0.428	0.431	0.435
Bus 68	52	0.448	0.450	0.452	0.456	0.459
	67	0.380	0.384	0.387	0.390	0.392
	68	0.348	0.352	0.355	0.357	0.360

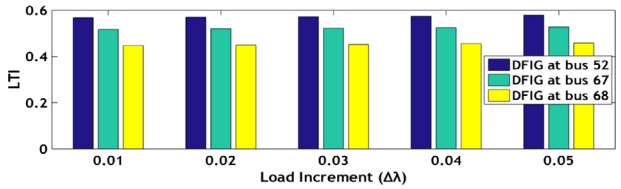

Fig. 5. LTI at load bus 52 for various wind farm locations.

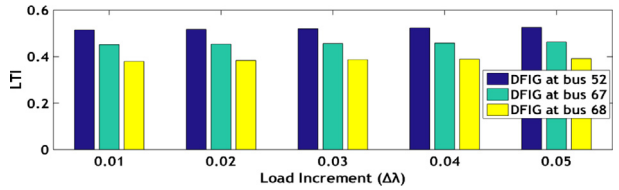

Fig. 6. LTI at load bus 67 for various wind farm locations.

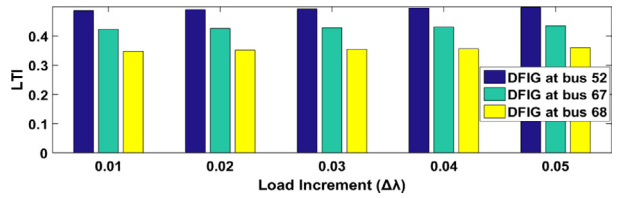

Fig. 7. LTI at load bus 68 for various wind farm locations.

stable when the wind farm is integrated at bus 68 compared to the other two locations. Thus, it can be said that bus 68 is the best location for the connection to the wind farm, among the three assumed possible locations.

The same study is carried out for the other three zones by assuming some available locations for wind farm integration in each zone. They are bus 56, bus 59, bus 60 in zone II, bus 26, bus 28, bus 29 in zone III and bus 33, bus 36, bus 61 in zone IV [16]. These nearby locations in each zone are chosen arbitrarily, since our main focus is to find the best location among a given set of possible locations for wind farm integration using LTI and the best locations are found to be bus 56 in zone II, bus 28 in zone III and bus 36 in zone IV.

4.2. Finding the optimum wind power penetration

The wind power penetration ($\%P$) is the ratio of total wind power entering the electric grid to the total amount of all existing loads ($\sum_{i=1}^{n} P_{Li}$), plus the additional load at the DFIG node [17]. The expression of $\%P$ is as shown in (6). For the 1000 MW DFIG based wind farm integrated with the 68-bus system, the penetration level was found to be 5.37%.

$$\%P = \frac{P_{dg}}{\sum_{i=1}^{n} P_{Li} + P_{dg}} * 100 \tag{6}$$

Here, the wind farm is integrated into the best location, i.e. bus 68 of zone-I, which is determined in the previous section. The output power can be varied by changing the number of turbine-generator sets. For each level of penetration, LTI is calculated on the load buses in the same fashion as said before and the LTI values are represented in Table 2. It can be observed that with the change in penetration level, the LTI values of the load buses are changing. It indicates that the system stability varies with change in penetration. When the wind power is increased from 500 MW to 1000 MW (corresponding to an increase in penetration from 2.76% to 5.37%), the LTI values are decreasing, which indicates an improvement in the system's stability. For a larger wind farm of capacity 2000 MW, it is seen that when the penetration is increased beyond 1500 MW (7.85% penetration), the LTI values start increasing, which indicates system stability degradation. This LTI variation can be clearly observed from the plots shown in Figs. 8 to 10. So, the optimum wind power penetration on bus 68 was found to be 1500 MW.

Table 2. LTI variation with a rise in wind-power penetration.

P_{dg} in MW ($\%P$)	LTI with different $\Delta\lambda$					
	Bus	$\Delta\lambda$				
		0.01	0.02	0.03	0.04	0.05
500(2.76)	52	0.487	0.490	0.492	0.495	0.499
	67	0.401	0.403	0.406	0.409	0.413
	68	0.361	0.364	0.366	0.369	0.373
700(3.82)	52	0.475	0.478	0.480	0.482	0.486
	67	0.385	0.387	0.390	0.394	0.397
	68	0.353	0.357	0.360	0.362	0.365
1000(5.37)	52	0.448	0.450	0.452	0.456	0.459
	67	0.380	0.384	0.387	0.390	0.392
	68	0.348	0.352	0.355	0.357	0.360
1500(7.85)	52	0.436	0.439	0.443	0.446	0.450
	67	0.366	0.369	0.372	0.374	0.378
	68	0.335	0.339	0.341	0.344	0.347
1600(8.32)	52	0.449	0.451	0.454	0.457	0.461
	67	0.380	0.382	0.385	0.387	0.391
	68	0.353	0.357	0.360	0.362	0.367
2000(10.19)	52	0.471	0.474	0.476	0.479	0.482
	67	0.392	0.394	0.397	0.401	0.404
	68	0.375	0.379	0.383	0.386	0.389

In a similar way, the study is repeated to find out the optimum wind power penetration in the other three zones by integrating the wind farm at the best location of respective zones and it is found to be 1800 MW (9.27%) at bus 56 of zone II, 1300 MW (6.87%) at bus 28 of zone III and 1600 MW (8.32%) at bus 36 of zone IV.

4.3. Voltage stability assessment with additional distributed load

Up to this point, the study was carried out considering the additional load connected to the DFIG terminal bus only. However, in practice, this additional load demand may be distributed among the nearby load buses in the

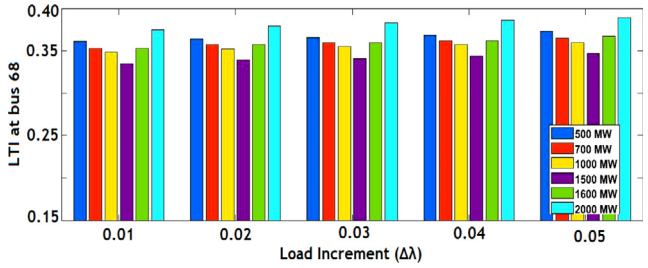

Fig. 8. LTI at bus 68 for various wind power penetrations.

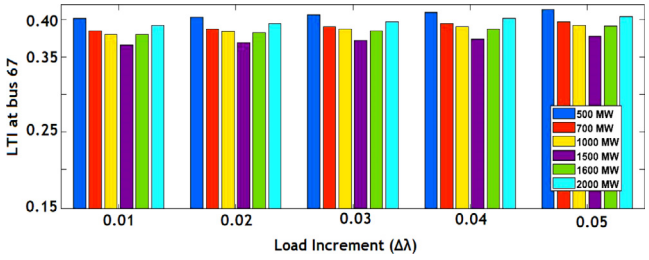

Fig. 9. LTI at bus 67 for various wind power penetrations.

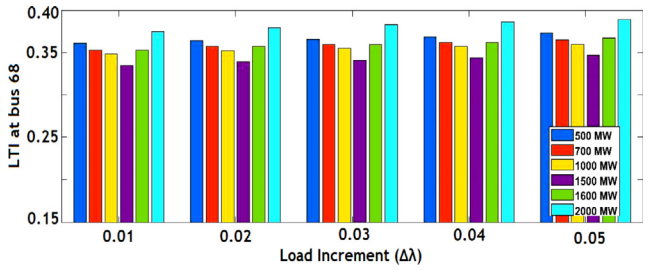

Fig. 10. LTI at bus 68 for various wind power penetrations.

system. So, in this section, we investigated system voltage stability with a distributed load case using LTI in both the 9-bus and 68-bus system.

4.3.1. Investigation on the WSCC 9-bus system

Considering the optimum wind power penetration (90 MW) on bus 8, the additional load is distributed among the three load buses of the nine-bus system using different distribution ratios [17,18]. The distribution is based on the fact that the DFIG terminal bus is having the greatest proportion of the additional load, and the rest is distributed among the other nearby buses under considerations as per the ratios shown in Table 3.

For each case of load distribution, the LTI is calculated on all the three load buses at 1% to 5% of the load increment ($\Delta\lambda$) as before and it is represented in Table 4. From the table, it may be noticed that the LTI values of the load buses vary with different load distribution cases, which indicates a variation in the system voltage stability. When the additional load is distributed according to distribution-1, we get lower LTI values on all three load buses than in the other two cases of load distribution, as shown by the LTI plots in Figs. 11 to 13. This implies the system is relatively more stable when the additional load demand is distributed as per distribution-1 (13:4:3).

4.3.2. Investigation on the 16-machine 68-bus system

In 68-bus system, for zone-I, considering the optimum wind power penetration (1500 MW) at bus 68, the 1500 MW additional load is distributed among the three nearby load buses (bus 52, bus 67, bus 68) following the same three distribution ratios as in the case of the 9-bus system. These different load distributions are shown

Table 3. Different load distributions.

Different distribution ratios	Bus 8	Bus 6	Bus 5
Distribution-1 (13:4:3)	59 MW	18 MW	13 MW
Distribution-2 (14:4:2)	63 MW	18 MW	9 MW
Distribution-3 (15:3:2)	68 MW	13 MW	9 MW

Table 4. LTI variation with different load distribution.

Load distribution	LTI with different $\Delta\lambda$					
	Bus	$\Delta\lambda$				
		0.01	0.02	0.03	0.04	0.05
Distribution-1	5	0.525	0.528	0.530	0.532	0.536
	6	0.416	0.418	0.421	0.423	0.426
	8	0.225	0.232	0.241	0.248	0.256
Distribution-2	5	0.542	0.548	0.553	0.559	0.563
	6	0.439	0.444	0.448	0.451	0.456
	8	0.269	0.274	0.282	0.288	0.293
Distribution-3	5	0.563	0.567	0.571	0.573	0.575
	6	0.488	0.491	0.493	0.496	0.499
	8	0.278	0.283	0.288	0.294	0.301

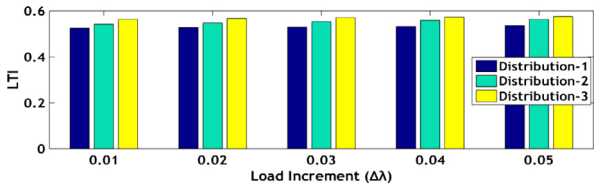

Fig. 11. LTI at lad bus 5 for various load distribution ratio.

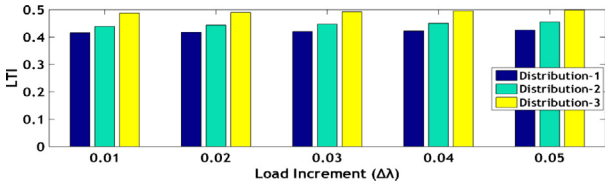

Fig. 12. LTI at lad bus 6 for various load distribution ratio.

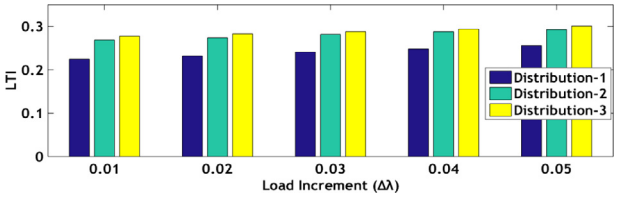

Fig. 13. LTI at lad bus 8 for various load distribution ratio.

Table 5. Different load distributions.

Type of distribution	Bus 68	Bus 52	Bus 67
Distribution-1(13:4:3)	975 MW	300 MW	225 MW
Distribution-2(14:4:2)	1050 MW	300 MW	150 MW
Distribution-3(15:3:2)	1125 MW	225 MW	150 MW

Table 6. LTI Variation with Different Load Distribution.

Load distribution	LTI with different $\Delta\lambda$					
	Bus	$\Delta\lambda$				
		0.01	0.02	0.03	0.04	0.05
Distribution-1	52	0.440	0.442	0.445	0.448	0.453
	67	0.395	0.398	0.402	0.404	0.406
	68	0.348	0.352	0.354	0.357	0.361
Distribution-2	52	0.461	0.464	0.466	0.470	0.473
	67	0.415	0.417	0.421	0.424	0.428
	68	0.372	0.374	0.378	0.381	0.384
Distribution-3	52	0.482	0.485	0.489	0.492	0.495
	67	0.431	0.434	0.436	0.439	0.443
	68	0.384	0.386	0.388	0.394	0.398

in Table 5. The LTI is calculated on the load buses in the same way for each case of load distribution, as shown in Table 6. This shows we are getting lower LTI values on the load buses when the load is distributed as per distribution-1 compared to distribution-2 and distribution-3. This is clear from the LTI plots, which are shown in Figs. 14 to 16. So, it can be said that we are getting comparatively more system stability for the distribution-1 case. This study with distributed additional load case is carried out in the other three zones in a similar way to find the best load distribution case from the system voltage stability point of view and it is found that we are getting relatively more system stability with distribution-1 (13:4:3) case compared to the other two cases of load distribution in each zone.

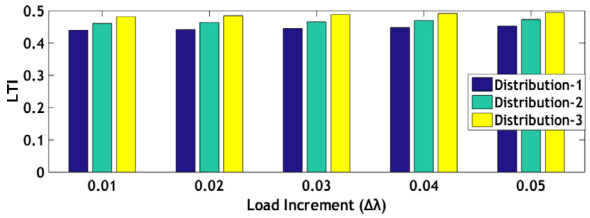

Fig. 14. LTI at load bus 52 for various load distribution ratio.

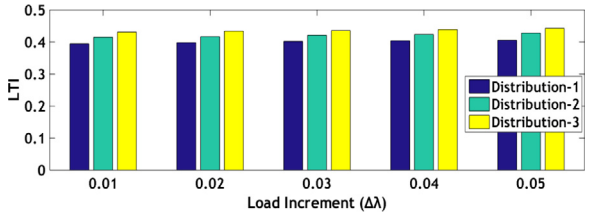

Fig. 15. LTI at load bus 67 for various load distribution ratio.

The overall findings of the present study are summarized in Table 7. All these findings are related to getting maximum voltage stability of the systems under consideration using LTI.

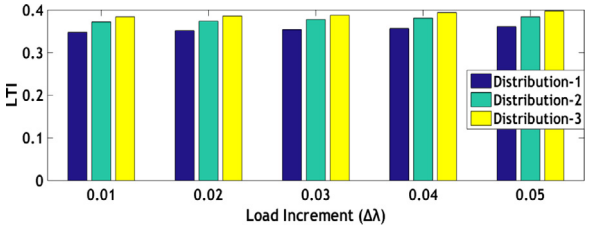

Fig. 16. LTI at load bus 68 for various load distribution ratio.

Table 7. The overall results of the investigations.

System under study		Assumed available points of connection	Best point of connection	Optimum wind power penetration	Best distribution ratio
9-bus system		Bus 5, Bus 6, Bus 8	Bus 8	90 MW (22.22%)	Distribution-1
68-bus system	Zone I	Bus 52, Bus 67, Bus 68	Bus 68	1500 MW (7.85%)	Distribution-1
	Zone II	Bus 56, Bus 59, Bus 60	Bus 56	1800 MW (9.27%)	Distribution-1
	Zone III	Bus 26, Bus 28, Bus 29	Bus 28	1300 MW (6.87%)	Distribution-1
	Zone IV	Bus 33, Bus 36, Bus 61	Bus 36	1600 MW (8.32%)	Distribution-1

Conclusions

The analysis of the impact of renewable energy penetration on system stability is one of the major concerns. The wide area monitoring system (WAMS)-based Local Thevenin Index (LTI) is a novel technique for assessing the voltage stability of power systems with renewable energy integration. This index aids in determining the best location for integrating the wind farm into the existing power system from the standpoint of grid voltage stability. This research examined the effects of the significant penetration of DFIG-based wind farms on the voltage stability of large power networks. We assessed the voltage stability for a DFIG integrated 16-machine 68-bus power network using LTI which can be collected from real-time PMU recording database. Owing to the largeness of the power system 68-bus system is divided in different zones from the proximity of buses. In each zone, the best location for wind farm integration and the optimum wind power penetration at that location is found out such that to achieve maximum voltage stability of the system. The study is also carried out considering a distributed additional load case in which three different distribution ratios are considered and the best ratio is found out from the system voltage stability point of view. This study was performed in the 9-bus system as well as in the 68-bus system in MATLAB platform.

Declaration of competing interest

The authors declare that they have no known competing financial interests or personal relationships that could have appeared to influence the work reported in this paper.

Acknowledgment

This work is a part of the AICTE-MHRD, the Government of India's quality improvement (QIP) program, through which academic professionals are sponsored for higher education.

References

[1] Chintakindi Raju, Mitra Arghya. PMU-based real-time load balancing strategy for lights-out case in India – a case study. In: First IEEE international conference on smart technologies for power, energy and control. Nagpur: IEEE PES; 2020, p. 5–10.

[2] Kalana Dulanjith Dharmapala, Rajapakse Athula, Krish Narendra, Zhang Yi. Machine learning based real-time monitoring of long-term voltage stability using voltage stability indices. IEEE Access 2020;8:222544–55.

[3] Reddy Amarsagar, Matavalam Ramapuram, Ajjarapu Venkataramana. Sensitivity based Thevenin index with systematic inclusion of reactive power limits. IEEE Trans Power Syst 2017;8950(c):1–10.

[4] Cutsem Thierry Van, Glavic Mevludin, Rosehart William, Canizares Claudio, Kanatas Marios, Lima Leonardo, et al. Test systems for voltage stability studies. IEEE Trans Power Syst 2020;35(5):4078–87.

[5] Pradhan Pradyumna, Chintakindi Raju, Mitra Arghya. WAMS based thevenin index for voltage stability assessment of power system integrated with wind farm. In: IEEE international conference for intelligent technologies. Hubballi, Karnataka: IEEE; 2021.
[6] Chintakindi Raju, Mitra Arghya. Execution of real-Time Wide Area monitoring system with big data functions and practices. In: PIICON 2020-9th IEEE power india international conference. Sonipat, India, India: IEEE.; 2020.
[7] Sumathi S, Ashok Kumar L, Surekha P. Solar PV and wind energy conversion systems. Springer International Publishing Switzerland; 2015.
[8] Vittal Vijay, Ayyanar Raja. Grid integration and dynamic impact of wind energy. New York: Springer; 2013, p. 1–152.
[9] Héctor Pulgar-Painemal. Enforcement of current limits in DFIG-based wind turbine dynamic models through capability curve. IEEE Trans Sustain Energy 2019;10(1):318–20.
[10] Zhu Yue. Power system loads and power system stability. Springer; 2020, http://dx.doi.org/10.1007/978-3-030-37786-1.
[11] Jing Ma, Zhang Yongxin, Shen Yaqi, Cheng Peng, Phadke AG. Equipment-level locating of low frequency oscillating source in power system with DFIG integration based on dynamic energy flow. IEEE Trans Power Syst 2020;35(5):3433–47.
[12] Qingxin Shi, Yuan Chen, Feng Wei, Liu Guangyi, Dai Renchang, Wang Zhiwei, et al. Enabling model-based LTI for large-scale power system security monitoring and enhancement with graph-computing-based power flow calculation. IEEE Access 2019;7:167010–8.
[13] Reddy Amarsagar, Matavalam Ramapuram, Ajjarapu Venkataramana. Validation of the sensitivity based thevenin index on large systems. In: IEEE power and energy society general meeting. Chicago, USA: IEEE; 2018.
[14] Adam Birchfield. New England 68-bus test system. Texas E & M Engineering Experiment Station; 2021.
[15] Mitra Arghya. Small signal stability analysis of power systems integrated with wind power using sensitivity-based index. Wind Eng 2019;45(1):35–49.
[16] Mitra Arghya, Chatterjee Dheeman. Active power control of dfig-based wind farm for improvement of transient stability of power systems. IEEE Trans Power Syst 2016;31(1):82–93.
[17] Fatnani Megha, Mitra Arghya. Small signal stability analysis of wind farm integrated multi-machine power system with distributed load. In: 8th International conference on power systems. (ICPS), Jaipur, India: IEEE; 2019.
[18] Wankhede Sumeet K, Mitra Arghya. Transient stability analysis of DFIG-based wind farm integrated power system with distributed loads. In: 7th international conference on power systems. ICPS, Pune, India: IEEE; 2017, p. 182–7.